JOURNAL OF GEOPHYSICAL RESEARCH, VOL. 101, NO. B5, PAGES 11,579–11,588, MAY 10, 1996

Remote sensing of volcanic ash clouds using special sensor microwave imager data

David J. Delene[1] and William I. Rose

Department of Geological Engineering and Sciences, Michigan Technological University, Houghton

Norman C. Grody

Microwave Sensing Group, NOAA Satellite Research Laboratory, Camp Springs, Maryland

Abstract. Measurements from the satellite-based special sensor microwave imager (SSM/I) were used to collect passive microwave radiation (19-85 GHz) for the August 19, 1992 (UT date), Crater Peak/Spurr volcanic cloud. This eruption was also imaged by a ground-based C-band radar system at Kenai, Alaska, 80 km away, and by the thermal infrared channels of the polar-orbiting advanced very high resolution radiometer (AVHRR). The SSM/I sensor detects scattering of Earth-emitted radiation by millimeter size volcanic ash particles. The size of ash particles in a volcanic ash cloud can be estimated by comparing the scattering at different microwave frequencies. The mass of particles in the volcanic ash cloud can be estimated by using a theoretical method based on Mie theory or by adapting the empirical methods used for estimating rainfall rates and accounting for the different dielectric constants of volcanic ash and raindrops. For the August 19, 1992, Crater Peak/Spurr eruption, the SSM/I-based estimate of ash fallout mass (1.3×10^9 - 3×10^{10} kg) was 4%-85% of the mass fallout measured in the field. Like weather radar systems, the SSM/I offers the ability to sense young volcanic ash clouds during and immediately following (within 30 min) actual eruptions. Because most volcanoes are out of range of weather radar systems, the SSM/I may be an important tool for determining the magnitude, initial trajectory, and potential fallout mass of eruptions. The SSM/I may therefore play a role in mitigating volcanic cloud hazards for aircraft, determining masses where ground sampling is not possible, and in issuing fallout warnings for communities downwind of volcanic eruptions.

Introduction

Volcanic ash clouds are now widely recognized as a significant hazard to aviation [*Casadevall*, 1994]. As a result, there is a considerable effort being expended by scientists to mitigate this hazard. This effort involves remote sensing of volcanic clouds by many ground-based and satellite sensors. Ground-based radar systems have been shown to be useful during and for up to 30 min following volcanic eruptions [*Harris and Rose*, 1983; *Rose et al.*, 1995a]; however, most volcanoes are out of range of modern radar systems, which are deployed near cities. Satellite-based ultraviolet sensors are used to study volcanic gas clouds [*Krueger et al.*, 1995], and infrared sensors are used to track and characterize volcanic ash clouds as they disperse in the atmosphere for up to several days after an eruption [*Schneider and Rose*, 1995]. However, near the volcanic vent, many volcanic ash clouds are opaque in the infrared region and appear similar to meteorological clouds [*Wen and Rose*, 1994]. As a result, infrared sensors, such as the advanced very high resolution radiometer (AVHRR), are of limited use in determining the particle size distribution and mass of these opaque volcanic ash clouds. This paper describes new techniques, based on the special sensor microwave imager (SSM/I), to estimate particle size and mass of the volcanic ash clouds that are opaque to infrared sensors and out of range of ground-based radar systems.

The SSM/I is a seven-channel, linearly polarized, passive microwave radiometric system which measures radiation at 19.35-, 22.235-, 37.10-, and 85.5-GHz [*Hollinger et al.*, 1987; *Hollinger*, 1989]. Note that there is no 22.235-GHz horizontally polarized channel. The instrument is a conically scanning radiometer which scans a 102^0 segment at an Earth incident angle of 53^0. The SSM/I instrument was first launched aboard the Defense Meteorological Satellite Program (DMSP) F8 satellite in July 1987. The 85-GHz channels failed within the first 2 years of operation thereby compromising the DMSP-F8 satellite's ability to study volcanic ash clouds. Fortunately, additional SSM/I instruments were launched in December 1990 and November 1991 aboard the DMSP-F10 and DMSP-F11 satellites, respectively. The instantaneous field of view of the SSM/I is elliptical, 13 x 15 km for the 85-GHz channels, 29 x 37 km for the 37-GHz channels, and 43 x 69 km for the 19-GHz channels. For a detailed description of the SSM/I and brightness temperature computations, readers are referred to the *Users Guide to the Special Sensor Microwave Imager (SSM/I) Data* which is available upon request from the Distributed Active Archive Center of the Marshall Space Flight Center.

The SSM/I was designed and built by the Department of Defense to aid in weather forecasting. However, passive

[1]Now at Department of Atmospheric Sciences, University of Wyoming, Laramie.

Paper number 96JB00643.
0148-0227/96/96JB-00643$09.00

microwave data have also been applied to land surface-type classification [*Neale et al.*, 1990], snow and sea ice studies [*Kunzi et al.*, 1976], and precipitation estimates [*Wilheit*, 1986]. Currently, researchers are using SSM/I data to study the global hydrological cycle [*Ferraro et al.*, 1994a].

The remote sensing of meteorological clouds and precipitation forms a good basis for the study of volcanic clouds because of the characteristics they share. Precipitation systems contain ice particles, which owing to their size and abundance, behave similarly to millimeter-sized silicate particles and possible ice-coated ash particles [*Rose et al.*, 1995b] found in volcanic clouds. Owing to these similarities, it is reasonable to assume that volcanic clouds can be studied using the methods developed for studying precipitation systems.

Although the SSM/I sensor was designed for meteorological applications, it has the potential of providing information about particle size and mass during and shortly after volcanic eruptions. The SSM/I instrument measures the Earth-emitted radiation at millimeter wavelengths, which makes it particularly useful for detecting the scattering from millimeter-sized particles. In this paper, we exploit the knowledge obtained from the study of meteorological clouds using SSM/I data and apply these methods to volcanic ash clouds. We present the results of applying SSM/I data to the study of the August 19, 1992 (UT date), eruption of Mount Spurr, Alaska.

Volcanic Ash Cloud Data

The SSM/I data archive was searched for possible detection of the recent eruptions of Mount Spurr, Lascar, Klyuchevskoi, and Rabaul. There was some evidence of the Mount Spurr, Klyuchevskoi, and Rabaul eruptions in the SSM/I data archive. There are several reasons why not all volcanic ash clouds are observed by the SSM/I instruments. (1) The SSM/I instrument has a 1400-km swath, which results in a single instrument only observing about 60% of the Earth in 24 hours. The interswath gaps vary from day to day resulting in changes in the area observed. (2) There are sometimes data gaps within the SSM/I orbits. (3) It may not be possible for microwaves to detect volcanic ash clouds older than about 0.5 hours owing to the rapid fallout rate of millimeter-sized particles [*Rose et al.*, 1995a].

This paper focuses on the volcanic cloud emitted from the August 19, 1992, subplinian eruption of the Crater Peak vent at the Mount Spurr volcano in south central Alaska. The reasons for selecting this volcanic cloud for study are the satisfactory SSM/I image (see Figure 1) and the complementary ground-based C-band radar and satellite-based AVHRR data. The SSM/I image captured the volcanic ash cloud during the middle of the eruption, which lasted between 0142 and 0510 UT [*Rose et al.*, 1995a]. Owing to the shorter wavelength, which is sensitive to smaller particles, and the better spatial resolution, the 85-GHz channel is best for detecting volcanic ash clouds.

When the SSM/I brightness temperature data were imported into a Terascan^{TM} software package, the data were found to suffer from navigational errors. These errors caused the land/water boundaries to be incorrect when overlaying the coast on an image. Therefore each SSM/I image was adjusted until the land/water boundaries of the map overlay coincided visually with the land/water boundaries of the SSM/I data. The selective nature of this process resulted in navigational error of as much as 5-10 km. *Ferraro and Marks* [1995] reported having similar (10-km) navigational errors with SSM/I data.

The Crater Peak/Spurr volcanic ash cloud was observed by weather radar to have a cloud top height of about 14 km [*Rose et al.*, 1995a]. On the basis of the total ozone mapping spectrometer SO_2 cloud-tracking and wind data, the SO_2 cloud altitude was estimated at 12-14 km [*Bluth et al.*, 1995]. Owing to the SSM/I 53^0 incidence angle, the volcanic cloud is offset in relation to its true map position. Therefore the volcanic cloud position must be adjusted using the satellite incident angle and cloud height to calculate its true surface location. Note that the AVHRR is a nadir viewing instrument, therefore it does not have such a distortion associated with it.

The adjusted position of the SSM/I volcanic ash cloud can be compared with that observed by radar and AVHRR (see Figure 2). The volcanic ash cloud area detected by the SSM/I instrument is larger than the area detected by C-band radar but smaller than the area detected by AVHRR. This is due to the fact that when the majority of the particles in the volcanic ash cloud are smaller than a minimum particle size, the instrument no longer detects the volcanic ash cloud. The minimum particle size detectable by an instrument is hard to quantify precisely because of the combined effects of the particle size distribution, the single-particle cross section, the different shapes of particles, and the specifications of the instrument. In our case, the minimum particle size for the SSM/I instrument is between 0.1 and 1 mm.

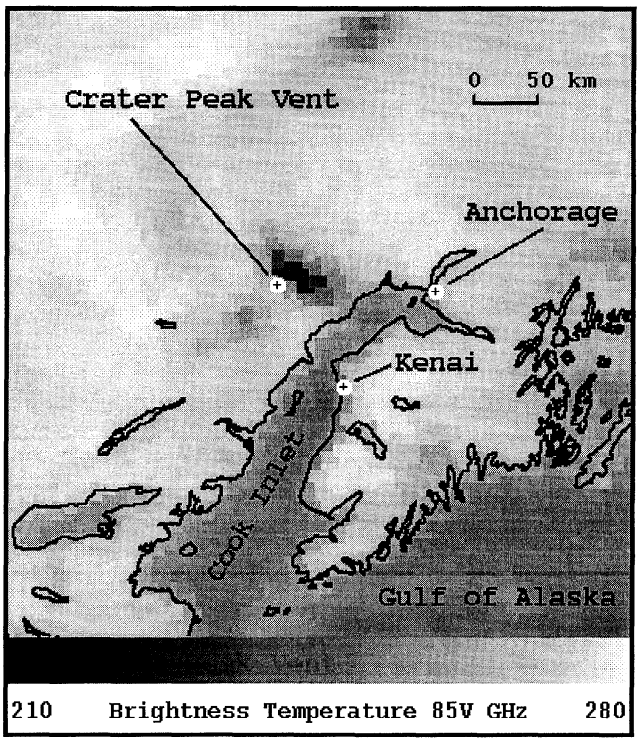

Figure 1. Special sensor microwave imager (SSM/I) 85-GHz (vertical polarization) image of the Cook Inlet area of south central Alaska, on August 19, 1992, at 0221 UT. The dark pixels east of the Crater Peak vent show the possible presence of the volcanic ash cloud. The image was registered using Lambert azimuthal map projection with 5x5 km pixels.

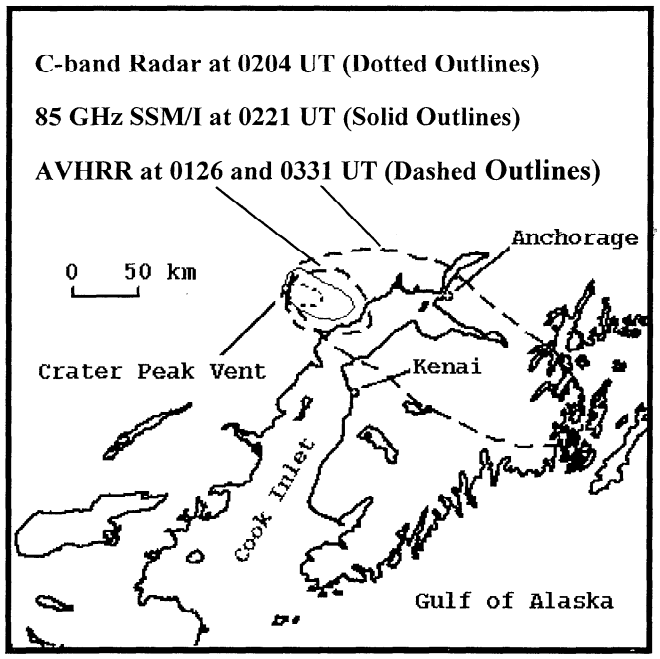

Figure 2. Extent of the August 19, 1992, Crater Peak/Spurr volcanic ash cloud as observed by C-band radar (5 cm), 85-GHz SSM/I (3.5 mm), and band 4 AVHRR (10.8 um). The outline of the volcanic ash cloud was subjectively determined by interpolating between volcanic ash cloud pixels and nonvolcanic cloud pixels based on volcanic ash cloud pixels having lower brightness temperatures than nonvolcanic cloud pixels.

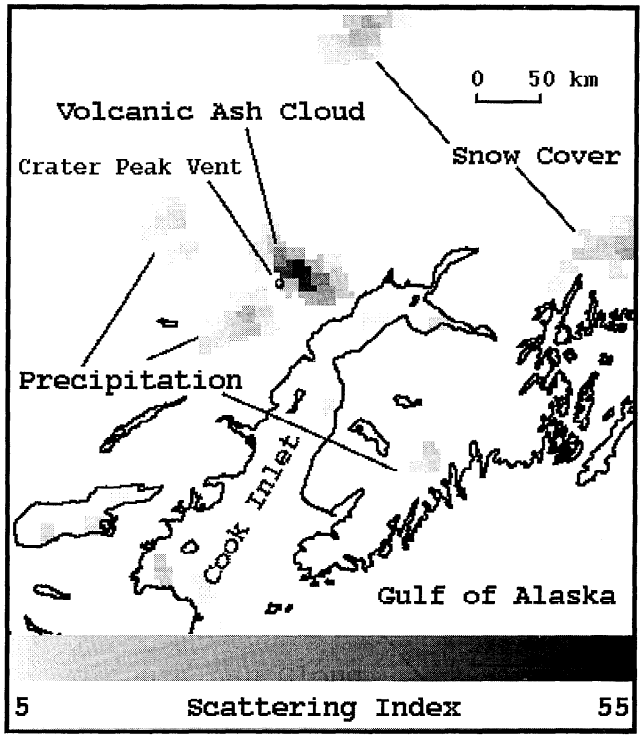

Figure 3. The scattering of radiation as observed by the SSM/I instrument on August 19, 1992, at 0221 UT. Precipitation and snow cover are classified using the current land surface equations [*Ferraro et al.*, 1994b].

Analysis of Volcanic Ash Clouds

Volcanic ash clouds can be analyzed by adapting methods developed for the study of precipitating systems. By employing these methods, the similarities and differences between volcanic ash clouds and other precipitation are developed.

SSM/I scenes can be separated in two classes: absorbing and volume-scattering materials [*Grody*, 1991]. Absorbing surfaces (water, melting snow, and vegetation) have brightness temperatures that increase with frequency, owing to the presence of water in these materials. In contrast, scatterers (dry snow cover, desert sand, and precipitation) have brightness temperatures that decrease with increasing frequency. Scattering areas on an SSM/I image occur where radiation has been emitted and then scattered by particles before being detected by the SSM/I sensor. In contrast, absorbing areas occur where radiation is emitted from a surface and not scattered before being detected by the SSM/I sensor.

Procedures have been developed and refined that use SSM/I data to compute a scattering index for the 85-GHz vertical polarization channel [*Grody*, 1991; *Fiore and Grody*, 1992; *Weng et al.*, 1994]. The scattering index is computed by using the low-frequency channels (19- and 22-GHz) to estimate the 85-GHz brightness temperature for nonscattering conditions and then subtracting the observed 85-GHz brightness temperature. The more radiation the area scatter, the higher the scattering index. The scattering index for the August 19, 1992, Crater Peak/Spurr volcanic ash cloud (see Figure 3) was computed by using the most recent land surface scattering formula [*Ferraro et al.*, 1994b]:

$$SI_L = 451.88 - 0.44T_b(19v) - 1.775T_b(22v) + 0.00574T_b(22v)^2 - T_b(85v) \quad (1)$$

where T_b is the SSM/I brightness temperature for the vertically polarized 19-, 22- and 85-GHz channels. The image of the scattering index shows that the volcanic ash cloud is a strong scatterer of radiation at a frequency of 85-GHz. A minimum scattering index of 5 K removes most of the background, whereas a threshold value of 10 K eliminates any false signatures (nonvolcanic cloud pixels). In global precipitation classifications, a threshold value of 10 K is used, however, for regional applications the threshold can be reduced [*Ferraro et al.*, 1994b]. By using the scattering index with a minimum threshold of 5 K, the edge of the volcanic ash cloud can be determined systematically instead of arbitrarily choosing the edge of the volcanic ash cloud based on the 85-GHz channel.

In addition to the volcanic ash cloud, Figure 3 also shows areas of high scattering due to snow cover and precipitation. Once an area has been identified as a scatterer, the equations, $T_b(22v)>264$ and $T_b(22v)>175+0.49T_b(85v)$ are used to distinguish whether scattering is due to precipitation or snow cover [*Ferraro et al.*, 1994b]. Dry snow cover acts as a scatterer because it contains ice particles separated by air spaces. These ice particles scatter the radiation emitted from the ground below. Precipitation clouds that contain ice particles also scatter the radiation emitted by the Earth's surface. A plot of the 85v versus 22v GHz channel for the

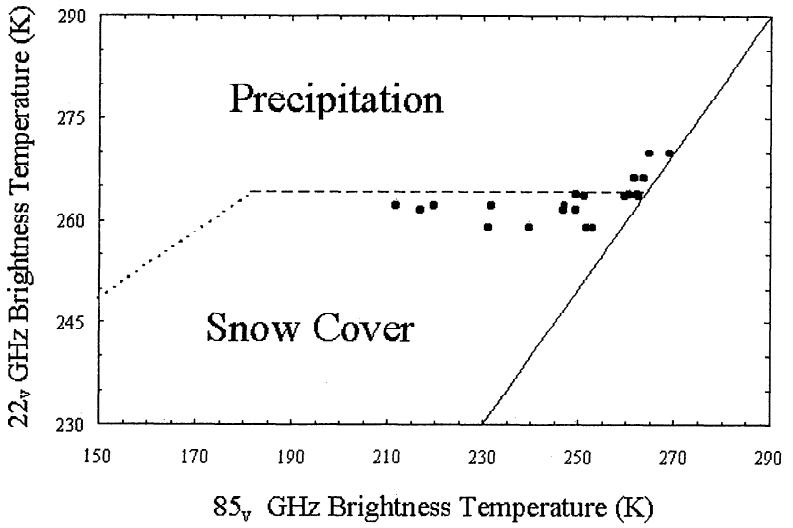

Figure 4. The solid circles are pixel values from the August 19, 1992, Crater Peak/Spurr volcanic ash cloud. The solid line denotes the separation between (left) scatterers and (right) absorbers. The dashed and dotted lines are based on empirical equations that are generally used to separate precipitation and snow cover [*Ferraro et al.*, 1994b].

August 19, 1992 Crater Peak/Spurr volcanic ash cloud (see Figure 4) shows that the volcanic ash cloud straddles the empirical boundary between precipitation and snow cover. In general, this makes it difficult to distinguish volcanic ash clouds from either snow cover or precipitation. However, for volcanic eruptions in areas without snow cover, it may be possible to distinguish volcanic ash clouds from precipitation. A good candidate for future study would be the 1991 eruption of Mount Pinatubo, Philippines.

In order to calculate the particle size distribution and mass of the volcanic ash clouds, it is important to determine the Earth's surface brightness temperature beneath the volcanic ash cloud. One approach is to use the brightness temperature of the pixels surrounding the volcanic ash cloud. It was found that the pixels surrounding the August 19, 1992, Crater Peak/Spurr volcanic ash cloud have brightness temperatures that vary by 5 K. This variation is mainly due to changes in emissivity. Another approach is to use the brightness temperature of the area 24 hours before the eruption. This assumes that the surface emissivity and temperature do not vary greatly between the two observations. To test this assumption in the vicinity of the August 19, 1992, Crater Peak/Spurr eruption, several SSM/I images from different days were compared to see how the brightness temperature changed in 24 hours. For our area of interest and time of year, it was found that the brightness temperature changed by less than 1 K. Therefore it seems that this assumption is reasonable and gives a smaller error than using the brightness temperature of the surrounding pixels. This prior observation method also has the advantage of having variable brightness temperatures underlying the volcanic ash cloud, which takes into account the changes in emissivity. Figure 5 compares the

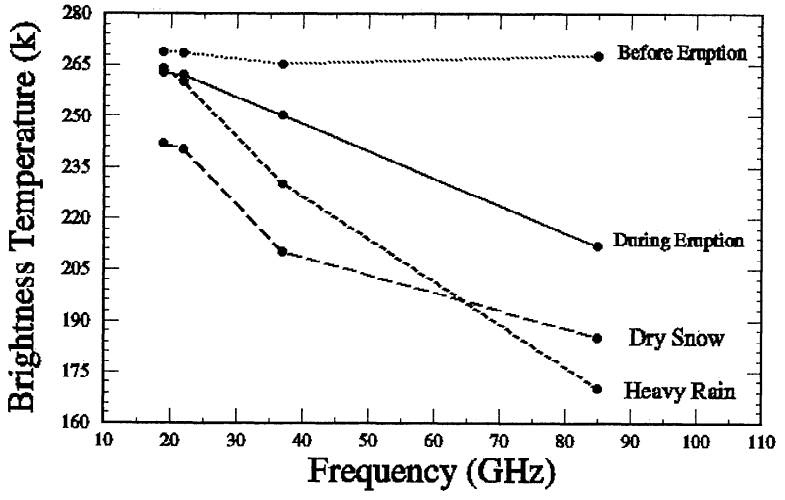

Figure 5. The SSM/I brightness temperature of the center of the August 19, 1992, Crater Peak/Spurr volcanic ash cloud as observed from the DMSP-F11 satellite at 0221 UT (during eruption). The same location as observed from the DMSP-F11 satellite on August 18, 1992, at 0232 UT (before eruption). Examples of dry snow and heavy rain are given for comparison [*Ferraro et al.*, 1994b]. Note that both snow and precipitation also have a wide range of values throughout the different SSM/I frequencies.

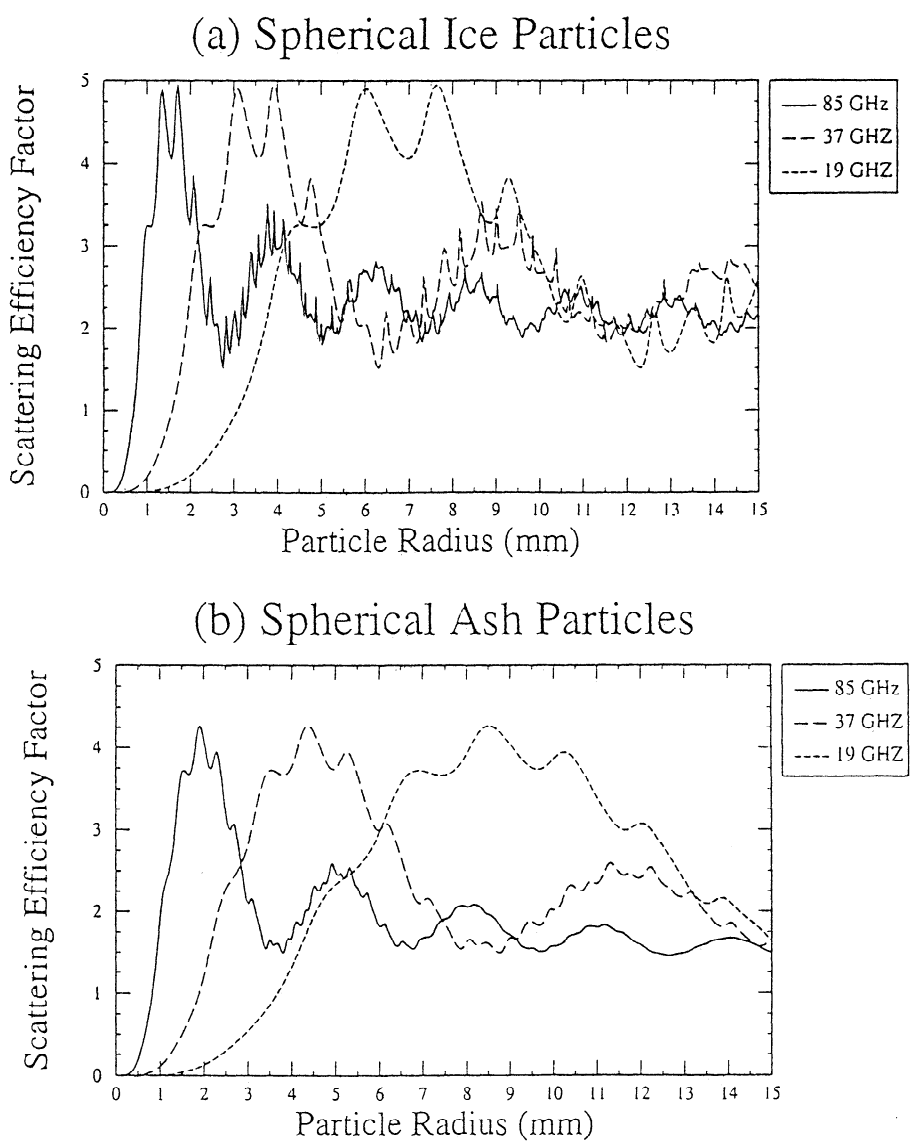

Figure 6. Scattering efficiency factor for spherical (a) ice and (b) ash particles as a function of radius. The index of refraction of ice [*Tiuri et al.*, 1984] is different than the index of refraction of volcanic ash [*Adams et al.*, 1996], which results in different scattering efficiency factors for ice and ash particles.

frequency dependence of brightness temperature for volcanic ash clouds, dry snow, and heavy rain. Also shown are the SSM/I brightness temperatures of the Mount Spurr area 24 hours preceding the eruption.

Determination of Silicate Particle Size Distribution

The low brightness temperatures of the volcanic ash cloud (see Figure 1) are the result of scattering of Earth-emitted radiation by ash particles. The scattered intensity for a single particle depends strongly on the ratio of the particle size to the wavelength of the incident radiation. This ratio defines two major types of scattering, Rayleigh and Mie scattering. If the incident wavelength is less than 1/10 of the particle size, the resulting scattering is defined as Rayleigh scattering. Mie scattering occurs when the incident wavelength is of the order of the particle size. *McCartney* [1976] and *van de Hulst* [1981] give in-depth discussions on the scattering of radiation by cloud particles.

Figure 6 shows the scattering efficiency factors for ice and ash particles. The efficiency factor is the ratio of the particle's cross section to its geometrical cross section. The total energy scattered in all directions is equal to the energy of the incident wave falling on the area of the particle's scattering cross section. Note that the differences in the magnitude of efficiency factors for ash and ice are due to the differences in the refractive index between ice and ash particles.

For the Rayleigh scattering region (i.e., 0.3 mm or smaller at 85-GHz), the efficiency factor is relatively small, which results in a small effect on the brightness temperature. The scattering efficiency factor does not become large until you enter the Mie region. The Mie region is from the upper end of the Rayleigh region until there is a constant efficiency factor. When two channels have the same scattering efficiency factor, the brightness temperature that they observe will be the same since they scatter Earth-emitted radiation in a similar fashion. This is possible in band 4 and band 5 of the AVHRR when observing a volcanic ash cloud with large (millimeter-sized) particles [*Lin and Coakley*, 1993].

Volcanic ash clouds contain a range of particle sizes, which can be described by a particle size distribution. Below we describe a simple radiative transfer model which determines the mean particle size and the mass of a volcanic ash cloud from SSM/I measurements. A more complex radiative transfer model would include emission by particles within the volcanic ash cloud [*Lin and Coakley*, 1993; *Prata*, 1989], but that is beyond the scope of this paper.

Assuming little absorption/emission by the volcanic ash cloud, the emerging brightness temperature (T_b) observed by the SSM/I satellite can be approximated by [*Grody and Basist*, 1994].

$$T_b(v) = \tau_{sc}(v) T_o \tag{2}$$

where τ_{sc} is the transmittance and T_o is the brightness temperature outside the volcanic ash cloud. Neglecting multiple scattering, the transmittance is

$$\tau_{sc}(v) = \exp(-L V_{sc}) \tag{3}$$

where L is the thickness of the cloud and V_{sc} is the volume scattering coefficient. The volume scattering coefficient is given by

$$V_{sc} = \int_0^\infty \pi r^2 Q_{sc}(r/\lambda) n(r) dr \tag{4}$$

where $n(r)$ is the particle size distribution, λ is the wavelength, and r is the particle radius. The scattering efficiency factor (Q_{sc}) for ice and ash particles are plotted in Figure 6. The scattering efficiency factors are computed using Mie theory [*Barber and Hill*, 1990]. Owing to the similarities between ice and ash scattering efficiency factors, it is difficult to distinguish ice from ash particles. As a consequence, it is difficult to determine if the SSM/I instrument is detecting ash particles or ice-coated particles without using supplementary data.

On the basis of aircraft sampling of volcanic ash clouds, a lognormal distribution is considered to be the most appropriate particle size distribution for volcanic ash clouds [*Farlow et al.*, 1981]. The normalized lognormal distribution has the following form:

$$N(r) = \frac{\exp\left\{-\dfrac{[\ln(r)-u]^2}{2\sigma^2}\right\}}{\sqrt{2\pi}\,\sigma\, r} \tag{5}$$

where r is the particle radius, u is the mean, and σ is the standard deviation. On the basis of volcanic ash cloud measurements, a standard deviation of 0.74 is used for the lognormal distribution [*Hobbs et al.*, 1991; *Wen and Rose*, 1994]. Therefore, for a given wavelength, the volume scattering coefficient is a function of the mean particle size. The transmittance of the cloud can be calculated from measurements of the volcanic ash cloud brightness temperature (T_b) and the brightness temperature below the cloud (T_o). By combining observations from two different channels, the number of particles and thickness of the volcanic ash cloud can be eliminated to give the following equation:

$$\frac{\ln(\tau_{sc}(v_1))}{\ln(\tau_{sc}(v_2))} = \frac{\int_0^\infty \pi r^2 Q_{sc}(r/\lambda_1) N(r)\, dr}{\int_0^\infty \pi r^2 Q_{sc}(r/\lambda_2) N(r)\, dr} \tag{6}$$

In (6), the frequencies and wavelengths are chosen to correspond to two of the channels of the SSM/I instrument. The left side of the equation is determined by the SSM/I observations of the volcanic ash cloud. On the right side, the normalized lognormal particle size distribution (5) is used with a standard deviation of 0.74, and the mean value of the particle size distribution is computed. The index of refraction value for ash particles in the Crater Peak/Spurr eruption [*Adams et al.*, 1996] was used in computing the scattering efficiency factor. The mean radius for the lognormal particle size distribution was found to be 0.9 mm using the 19- and 37-GHz channels and 0.3 mm using the 37- and 85-GHz channels.

These values of mean particle size seem reasonable when considering that C-band radar has the most intense reflection for particles ranging in radius from 1-10 mm [*Rose et al.*, 1995a]. The size of the SSM/I sensed volcanic ash cloud is larger than the size of the volcanic ash cloud detected by C-band radar; therefore the size of the particles that the SSM/I detects should be smaller. For the August 19, 1992, Crater Peak/Spurr eruption, theoretical calculations indicate that spherical ash particles with a radius of 0.5 mm fall out within about half an hour [*Rose et al.*, 1995a]. Therefore, for volcanic eruptions similar in size to the August 19, 1992, Crater Peak/Spurr eruption, the SSM/I instrument can only detect the volcanic ash cloud for about half an hour after the end of an eruption.

Mass Calculation of Silicate Particles

Two different methods for estimating the total volume and mass of ash in an eruption are developed using SSM/I data. The first method is based on the simple theoretical radiative transfer model outlined in the previous section. The second is an empirical method which relates the scattering index to an ashfall rate. The empirical method comes close to estimating the mass determined by field measurements of the actual ash deposits [*Neal et al.*, 1995]. Table 1 contains estimates of the total volume and mass for the August 19, 1992, Crater Peak/Spurr volcanic ash cloud based on these methods along with an estimate based on ground sampling of the ashfall blanket.

Table 1. Total Estimated Volumne and Mass of the August 19, 1992, Crater Peak/Spurr Volcanic Ash Cloud as Determined by the Two Methods Outlined in This Paper

	Channel	Volume, m^3	Mass, kg
Theoretical Method	85 GHz	5.1×10^5	1.3×10^9
	37 GHz	7.4×10^5	1.9×10^9
	19 GHz	1.7×10^6	4.5×10^9
Empirical Method		1.2×10^7	3.0×10^{10}
Ground Sampling		1.4×10^7	3.6×10^{10}

Both methods assume a constant eruption rate and that the eruption lasted for 3.5 hours. The extent of the volcanic ash cloud was determined by using a scattering index threshold value of 10. The theoretical method uses a lognormal particle distribution with a mean of 0.9 mm, a standard deviation of 0.74, and a particle fall out time of half an hour. The empirical method is based on the modified rainfall rate. The estimated volume and mass based on ground sampling of the ashfall blanket is from *Neal et al.* [1995].

Table 2. Radar Reflectivity for Center of August 19, 1992, Crater Peak/ Spurr Volcanic Ash Cloud

	Reflectivity, dBZ
SSM/I scattering index	
Rain drops	40.4
Ash particles	17.0
C-band radar, observation	20-30

The rain fall rate is based on stratiform rain. The ashfall rate uses a correction factor of 0.42

Theoretical Method

Once the mean value of the lognormal distribution is determined, it is possible to calculate the mass of the volcanic ash cloud using (2) if we assume that the particle size distribution is constant for the entire detected volcanic ash cloud and that the decrease in transmissivity is due only to the volcanic ash cloud. It is important to recognize that this method of calculating the mass of the volcanic ash cloud only estimates the amount of ash in the air at the time of observation. To estimate the total mass, we make use of the following: (1) theoretical calculations for the August 19, 1992, Crater Peak/Spurr eruption show that spherical ash particles with a radius of 0.5 mm would fallout within a half hour [*Rose et al.*, 1995a]; (2) the eruption lasted for 3.5 hours [*Eichelberger et al.*, 1995; *Rose et al.*, 1995a]; and (3) a constant eruption rate. Therefore, to estimate the total mass, the instantaneous mass of the cloud would have to be multiplied by a factor of 7 for the August 19, 1992, Crater Peak/Spurr eruption.

Empirical Method

The scattering index can be used to estimate the rainfall rate once an area has been classified as precipitation. The current empirical equation used to calculate the rainfall rate (millimeters per hour) from the scattering index (*SI*) over land surfaces is given as follows [*Ferraro and Marks*, 1995]:

$$R = 0.0051 SI^{1.947} \tag{7}$$

A similar empirical relationship could be developed to relate the scattering index to an ashfall rate. For the development of such a relationship, however, it would be necessary to have several SSM/I observations along with "ground truth" information about the ashfall rate. These types of data are not available at present; therefore we decided instead to use dielectric data to modify the rainfall rate equation to give an estimate of the ashfall rate. The radar return from an ash particle is less than that from a water particle. A correction factor (alpha) can be computed owing to the difference index of refraction of water and ash. The refractive index factors for ash and water are 0.39 and 0.93, respectively [*Rose and Kostinski*, 1991; Adams et al., 1996]. On the basis of only the different refractive index factors, the correction factor for radar reflectivity would be 0.42. Assuming that the change in refractive index has a similar effect on the scattering index as on radar returns, the alpha correction factor can be applied to (7) to give an ashfall rate.

Support for the use of this alpha correction factor is found when it is applied to calculating radar reflectivity of the volcanic ash cloud based on the scattering index. For stratiform (widespread, relatively uniform) rain the following empirical equation relates the reflectivity factor (Z) to the rainfall rate [*Skolnik*, 1990].

$$Z = 200 R^{1.6} \tag{8}$$

By combining (7) and (8), the radar reflectivity for a meteorological cloud can be calculated based on the SSM/I scattering index. Table 2 compares this value to that of the observed reflectivity and to the reflectivity using the alpha correction factor. The reflectivity based on stratiform rain is higher than that observed by radar, whereas the corrected reflectivity agrees better with the ground-based C-band radar observation.

Figure 7 shows the results of applying the modified rainfall relationship to the SSM/I data. The eruption rate was assumed to be constant and the eruption duration is assumed to be 3.5 hours [*Eichelberger et al.*, 1995; *Rose et al.*, 1995a]. Once the ash thickness is determined, the areal extent of the SSM/I pixel can be used to calculate the total volume of the eruption. For the Crater Peak/Spurr eruption a density of 2600 kg/m^3 can be assumed [*Neal et al.*, 1995], and the total mass of the volcanic ash cloud can be calculated.

Discussion

There are several reasons why methods outlined in this paper may incorrectly estimate the mass of the volcanic ash cloud: (1) the spatial resolution of the SSM/I instrument results in mixed pixel problems. The pixels at the edge of the volcanic ash cloud are only fractionally composed of the volcanic ash cloud which results in higher brightness temperatures than if they were completely filled. (2) The ash particles are assumed to behave like spherical particles which may be incorrect [*Heiken and Wohletz*, 1985]. (3) Some of the mass of the volcanic ash cloud is contained in particles which are too small for the SSM/I instrument to detect. (4) The ash emission rate probably is not constant [*Neal et al.*, 1995]. The theoretical method also has the problem of determining the atmospheric residence time of ash particles, which is necessary to be able to calculate the total mass of the volcanic ash cloud from a single observation. Determining the fallout time is difficult since there is a distribution of particle sizes which results in a distribution of particle atmospheric residence times.

The theoretical method uses many assumptions to simplify the mass calculation. One simplification is the assumption that scattering is dominant. By comparing the brightness temperature of the opaque region (214 K), as observed by the AVHRR, with that of the center of the volcanic ash cloud observed by the 85-GHz channel of the SSM/I (211 K), one may conclude that the 85-GHz SSM/I channel is sensing emission from the volcanic ash cloud. This would then imply that scattering is not dominant. However, when comparing the volcanic ash cloud spectrum in Figure 5 with that of a theoretical emission spectrum (see Figure 8), the volcanic ash cloud spectrum has a much sharper falloff with frequency. For the emission spectrum, the 19- and 37-GHz channels have brightness temperatures colder than the cloud-free case, whereas for the volcanic ash cloud, the 19- and 37-GHz channels do not show much of a change from the cloud-free case. Owing to the difference between the volcanic ash cloud spectrum and the theoretical emission spectrum, we believe

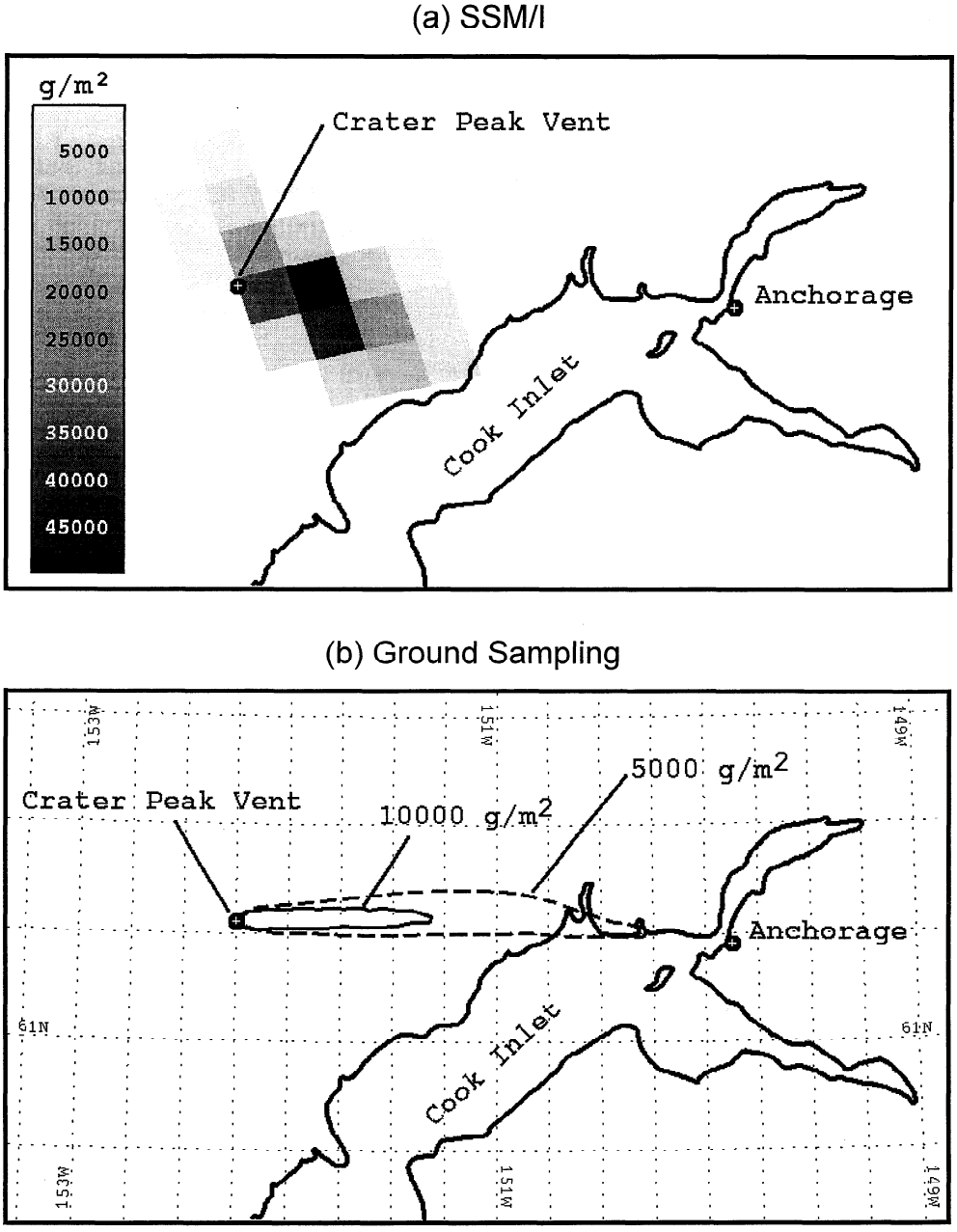

Figure 7. Selected isomass contours (g/m^2) of the August 19, 1992, Crater Peak/Spurr volcanic ash cloud as estimated from (a) SSM/I data using the modified rain fall rate equation and (b) ground sampling of the ashfall blanket (R. G. McGimsey, personal communication, 1995). Each SSM/I pixel is about 12.5 x 12.5 km. Some of the pixels to the north and northwest may be due to scattering by snow instead of the volcanic ash cloud. The difference observed between the SSM/I data and the ground sampling data may be due to a wind shear.

that the 85-GHz channel is dominated by scattering and not by emission. Another possible oversimplification in the theoretical method is the assumption of no multiple scattering, which is only true for low optical depths. This assumption requires further investigation to ascertain its importance.

Another potential source of error in calculating the volcanic ash cloud mass is due to the determination of the areal extent of the volcanic ash cloud. A microwave detector with a higher spatial resolution or a deconvolution scheme [*Farrar et al.*, 1994] can be used to reduce this error. Many other improvements can be made to the basic models presented in this paper for determining particle size and mass of volcanic ash clouds, however, the low spatial resolution and instantaneous view will still be major difficulties to overcome.

It is difficult to quantitatively describe the errors in the mass calculations from this single case study. Further development of the theoretical method will be necessary to produce reliable results with acceptable errors. For the empirical method, an idea of its error can be obtained by looking at the scattering index value. The center of the Crater

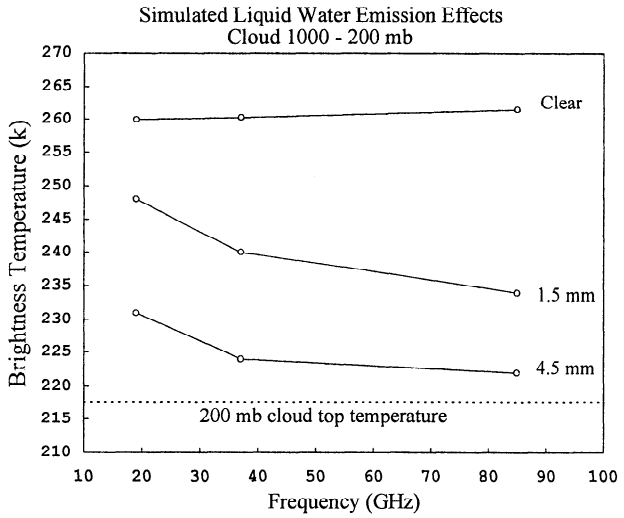

Figure 8. This simulation illustrates the type of spectrum one gets from liquid water emission alone. It is unrealistic to consider liquid drops up to 200 mbars, however, the point is that the emission signal does not have as sharp a drop-off with frequency as scattering. Comparing this emission spectrum to that of the volcanic ash cloud spectrum (see Figure 5), the volcanic ash cloud spectrum would be consistent with a scattering spectrum and not an emission spectrum.

Peak/Spurr volcanic ash cloud has a scattering index of about 55, which corresponds to an ash fall of 46,749 g/m^2. It seems reasonable to assume that the error in the scattering index is equal to or less than the threshold value ($SI_{error} \leq 10$). For a scattering index of 45, the ash fall is reduced to 35,752 g/m^2. This gives an idea of the upper limit on the empirical method error; however, the only good way to evaluate this error is to do several case studies of volcanic ash clouds.

Currently, meteorologists are developing and deploying new satellite sensors to extend their data coverage in both time and space to enable study of the global hydrological cycle. Many of these sensors will improve our ability to study volcanic ash clouds in the microwave portion of the spectrum. The Tropical Rainfall Measuring Mission satellite will have a microwave imager and precipitation radar [*Weinman et al.*, 1994]. The microwave imager is similar to the SSM/I with an improved horizontal resolution of 5 km. These sensors and other future satellites will improve our ability to estimate mass and ash fallout of volcanic clouds. Modern ground-based radar has some advantages over satellite-based microwave sensors; however, most volcanoes are not in the range of ground-based radar. By using ground-based radar to calibrate and verify microwave sensors, the study of volcanic ash clouds in the microwave region can be conducted on a global scale.

In the future, microwave satellite detectors could be used in real-time detection of volcanic ash clouds. Knowledge of both the size and trajectory of volcanic clouds are very important for hazard mitigation of volcanic eruptions. Once a volcanic cloud is detected, its trajectory, along with an estimate of the eruption magnitude and amount of ash fallout, could be used in the warning of aircraft and the nearby population. Microwave sensors, such as the SSM/I, have the limitation of only detecting young volcanic clouds, however, they complement other sensors, such as the AVHRR. Since the SSM/I is on a different satellite than the AVHRR, it provides detection of volcanic ash clouds at different times. By including the SSM/I sensor as a hazard mitigation tool, the chance of early satellite detection of volcanic clouds is improved.

Conclusions

If SSM/I data can be collected during an explosive, ash-producing eruption or within 30 min of its termination, it provides information similar to ground-based meteorological systems, which are rarely in the range of active volcanoes. From the SSM/I data, a scattering index can be quickly computed, and a threshold of 5-10 K can be used to define the volcanic ash cloud. SSM/I data can be used to estimate the particle size distribution and mass of volcanic ash clouds. The trajectory and shape of the volcanic ash cloud can be determined if corrections for navigational errors and incidence angle are made. Also, SSM/I data can be used to forecast the amount of ash fallout. In the case of the August 19, 1992, Crater Peak/Spurr eruption, the SSM/I data estimated the volcanic ash cloud mass to be 0.13-3.0 x 10^{10} kg, about 4%-85% of the mass determined from the field measurements of the ashfall blanket. Another important application for SSM/I data is to provide a means of estimating ash volume when the fallout occurs over an ocean. SSM/I data can provide useful information for volcanological use as well as hazard mitigation.

Acknowledgments. Special thanks go to Rob Bauer of the National Snow and Ice Data Center for his time, effort, and advice in obtaining data for this research. The SSM/I data were supplied in a straightforward and timely fashion by the Marshall Space Flight Center (MSFC) Distributed Active Archive Center (DAAC). The C-band radar data were supplied by Lee Kelley of the National Weather Service, Anchorage, Alaska. The Mie program for calculating the efficiency factors for a single spherical particle was supplied by W. J. Lentz. This research was aided by interaction with Jim Weinman and Alex Kostinski. Special thanks go to Ralph Ferraro of the Microwave Sensing Group, NOAA/Satellite Research Lab, for supplying reference materials and comments. Thanks to all the people that reviewed and commented on the paper, particularly Gregg Bluth and Christina Neal. Funding was provided by NASA through the Volcano/Climate program and the COMET program of NOAA.

References

Adams, R., W. F. Perger, W. I. Rose, and A. B. Kostinski, Measurements of the complex dielectric constant of volcanic ash from 4 to 19 GHz, *J. Geophys. Res.*, in press, 1996.

Barber, P. W., and S. C. Hill, Light scattering by particles: *Computational Methods*, 261 pp., World Sci., River Edge, N.I., 1990.

Bluth, G. J. S., C. J. Scott, I. E. Sprod, C. C. Schnetzler, A. J. Krueger, and L. S. Walter, Explosive SO_2 emission from the 1992 eruptions of Mount Spurr, Alaska, *U.S. Geol. Surv. Bull., B-2139*, 37-46, 1995

Casadevall, T. J., Volcanic ash and aviation safety: Proceedings of the first international symposium on volcanic ash and aviation safety, *U.S. Geol. Surv. Bull., 2047*, 1-450, 1994.

Eichelberger, J. C., T. E. C. Keith, T. P. Miller, and C. I. Nye, The 1992 eruptions of Crater Peak Vent, Mount Spurr volcano, Alaska: Chronology and summary, *U.S. Geol. Surv. Bull., 2139*, 1-18, 1995.

Farlow, H. N., V. R. Oberbeck, K. G. Snetsinger, G. V. Ferry, G. Polkowski, and D. M. Hayes, Size distributions and mineralogy of ash particles in the stratosphere from eruptions of Mount St. Helens, *Science*, *211*, 832-834, 1981.

Farrar, M. R., E. A. Smith, and X. Xiang, The impact of spatial resolution enhancement of SSM/I microwave brightness temperatures on rainfall retrieval algorithms, *J. Appl. Meteorol.*, *33*, 313-333, 1994.

Ferraro, R. R., and G. F. Marks, The development of SSM/I rain-rate retrieval algorithms using ground-based radar measurements, *J. Atmos. Oceanic Technol.*, *25*, 755-770, 1995.

Ferraro, R. R., N. Grody, D. Forsyth, R. Carey, A. Basist, J. Janowiak, F. Weng, G. F. Marks, and R. Yanamandra, Microwave measurements produce global climatic hydrologic data, *Eos Trans. AGU*, *75*, 337-338, 1994a.

Ferraro, R. R., N. C. Grody, and G. F. Marks, Effects of surface conditions on rain identification using the DMSP-SSM/I, *Remote Sens. Rev.*, *11*, 194-209, 1994b.

Fiore, J. V., and N. C. Grody, Classification of snow cover and precipitation using SSM/I measurements: Case studies, *Int. J. Remote Sens.*, *13*, 3349-3361, 1992.

Grody, N. C., Classification of snow cover and precipitation using the special sensor microwave imager, *J. Geophys. Res.*, *96*, 7423-7435, 1991.

Grody, N. C., and A. N. Basist, Snow cover identification using the special sensor microwave imager, *East. Snow Conf. 51st*, pp. 67-74, Dearborn, Michigan, 1994.

Harris, D. M., and W. I. Rose, Estimating particles sizes, concentrations, and total mass of ash in volcanic clouds using weather radar, *J. Geophys. Res.*, *88*, 10,969-10,983, 1983.

Heiken, G., and K. Wohletz, *Volcanic Ash*, 245 pp., Univ. of Calif. Press, Berkeley, 1985.

Hobbs, P. V., L. F. Radke, J. H. Lyons, R. J. Ferek, and D. J. Coffman, Airborne measurements of particle and gas emissions from the 1990 volcanic eruptions of Mount Redoubt, *J. Geophys. Res.*, *96*, 18,735-18,752, 1991.

Hollinger, J., DMSP Special Sensor Microwave/Imager calibration/validation, final report, vol. 1, Nav. Res. Lab., Washington, D. C., 1989.

Hollinger, J., R. Lo, G. Poe, R. Savage, and J. Peirce, *Special Sensor Microwave/Imager Users' Guide*, 120 pp., Nav. Res. Lab., Washington, D. C., 1987.

Krueger, A. J., L. S. Walter, P. K. Bhartia, C. C. Schnetzler, N. A. Krotkov, I. Sprod, and G. J. S. Bluth, Volcanic sulfur dioxide measurements from the total ozone mapping spectrometer instruments, *J. Geophys. Res., 100*, 14,057-14,076, 1995.

Kunzi, K. F., A. D. Fisher, and D. H. Staelin, Snow and ice surfaces measured by the Nimbus 5 microwave spectrometer, *J. Geophys. Res.*, *81*, 4965-4980, 1976.

Lin, X., and J. A. Coakley, Retrieval of properties for semitransparent clouds from multispectral infrared imagery data, *J. Geophys. Res.*, *98*, 18,501-18,514, 1993.

McCartney, E. J., *Optics of the Atmosphere Scattering by Molecules and Particles*, 408 pp., John Wiley, New York, 1976.

Neal, C. A., R. G. McGimsey, C. A. Gardner, M. L. Harbin, and C. J. Nye, Tephra-fall deposits from the 1992 eruptions of Crater Peak, Spurr volcano, Alaska: A preliminary report on distribution, stratigraphy, and composition, *U.S. Geol. Surv. Bull., 2139*, 65-80, 1995.

Neale, C. M. U., M. J. McFarland, and K. Chang, Land-surface-type classification using microwave brightness temperatures from the special sensor microwave/imager, *IEEE Trans. Geosci. Remote Sens.*, *28*, 829-837, 1990.

Prata, A. J., Infrared radiative transfer calculations for volcanic ash clouds, *Geophys. Res. Lett.*, *16* (11), 1293-1296, 1989.

Rose, W. I., and A. B. Kostinski, Radar remote sensing of volcanic clouds, *U.S. Geol. Surv. Bull. 2047*, 391-396, 1991.

Rose, W. I., A. B. Kostinski, and L. Kelley, Real time C-band radar observations of 1992 eruption clouds from Crater Peak/Spurr volcano, Alaska, *U.S. Geol. Surv. Bull., 2139*, 19-26, 1995a.

Rose, W. I., D. J. Delene, D. J. Schneider, G. J. S. Bluth, A. J. Krueger, I. Sprod, C. McKee, H. L. Davies, and G. G. J. Ernst, Ice in the 1994 Rabaul eruption cloud: Implications for volcano hazard and atmospheric effects, *Nature*, *375*, 477-479, 1995b.

Schneider, D. J., and W. I. Rose, Tracking of 1992 Crater Peak/Spurr eruption clouds using AVHRR, *U. S. Geol. Surv. Bull., 2139*, 27-36, 1995.

Skolnik, M. I., *Radar Handbook*, McGraw-Hill, New York, 1990.

Tiuri, M. E., A. H. Sihvola, E. G. Nyfors, and M. T. Hallikaiken, The complex dielectric constant of snow at microwave frequencies, *IEEE J. Oceanic Eng.*, *OE-9*, 377-382, 1984.

van de Hulst, H. C., *Light Scattering by Small Particles*, 470 pp., Dover, Mineola, N. Y., 1981.

Weinman, J. A., J. L. Schols, and L. S. Chiu, Precipitation distributions from combined airborne microwave radiometric/radar measurements and ground based VLF SFERICS observations in support of NASA's Tropical Rainfall Measuring Mission, in *Global Precipitation and Climate Change*, *NATO ASI Ser., Ser.. I*, *26*, 435-452, 1994.

Wen, S., and W. I. Rose, Retrieval of sizes and total masses of particles in volcanic clouds using AVHRR bands 4 and 5, *J. Geophys. Res.*, *99*, 5421-5431, 1994.

Weng, F., R. R. Ferraro, and N. C. Grody, Global precipitation estimations using defense meteorological satellite program F10 and F11 Special Sensor Microwave Imager data, *J. Geophys. Res.*, *99*, 14,493-14,502, 1994.

Wilheit, T. T., Some comments on passive microwave measurement of rain, *Bull. Am. Meteorol. Sci.*, *67*, 1226-1232, 1986

D. J. Delene, Department of Atmospheric Sciences, University of Wyoming, P.O. Box 3038, Laramie, WY 82071-3038. (e-mail: delene@omah.uwyo.edu)

N. C. Grody, Microwave Sensing Group, Satellite Research Laboratory, NOAA, Routing Code E/RA 12, 5200 Auth Road, Room 712, Camp Springs, MD 20746.

W. I. Rose, Department of Geological Engineering and Sciences, Michigan Technological University, 1400 Townsend Drive, Houghton, MI 49931. (e-mail: raman@mtu.edu)

(Received October 16, 1995; revised January 19, 1996; accepted February 13, 1996.)